tvst

https://doi.org/10.1167/tvst.7.5.33

Article

Retinotopic Responses in the Visual Cortex Elicited by Epiretinal Electrical Stimulation in Normal and Retinal Degenerate Rats

Kiran Nimmagadda[1,2] and James D. Weiland[3,4]

[1] Neuroscience Graduate Program, University of Southern California, Los Angeles, CA, USA
[2] USC – Caltech MD/PhD Program, Los Angeles, CA, USA
[3] Department of Biomedical Engineering, The University of Michigan, Ann Arbor, MI, USA
[4] Department of Ophthalmology and Visual Sciences, The University of Michigan, Ann Arbor, MI, USA

Correspondence: James D. Weiland, The University of Michigan, Biomedical Engineering and Ophthalmology, 2200 Bonisteel Blvd, 1107 Carl A. Gerstacker Building, Ann Arbor, MI 48109, USA. e-mail: weiland@umich.edu

Received: 12 February 2018
Accepted: 24 August 2018
Published: 31 October 2018

Keywords: electrical stimulation; cortical electrophysiology; retinotopy; rat; retinitis pigmentosa

Citation: Nimmagadda K, Weiland JD. Retinotopic responses in the visual cortex elicited by epiretinal electrical stimulation in normal and retinal degenerate rats. Trans Vis Sci Tech. 2018;7(5):33, https://doi.org/10.1167/tvst.7.5.33

Purpose: Electronic retinal prostheses restore vision in people with outer retinal degeneration by electrically stimulating the inner retina. We characterized visual cortex electrophysiologic response elicited by electrical stimulation of retina in normally sighted and retinal degenerate rats.

Methods: Nine normally sighted Long Evans and 11 S334ter line 3 retinal degenerate (*rd*) rats were used to map cortical responses elicited by epiretinal electrical stimulation in four quadrants of the retina. Six normal and six *rd* rats were used to compare the dendritic spine density of neurons in the visual cortex.

Results: The *rd* rats required higher stimulus amplitudes to elicit responses in the visual cortex. The cortical electrically evoked responses (EERs) for both healthy and *rd* rats show a dose-response characteristic with respect to the stimulus amplitude. The EER maps in healthy rats show retinotopic organization. For *rd* rats, cortical retinotopy is not well preserved. The neurons in the visual cortex of *rd* rats show a 10% higher dendritic spine density than in the healthy rats.

Conclusions: Cortical activity maps, produced when epiretinal stimulation is applied to quadrants of the retina, exhibit retinotopy in normal but not *rd* rats. This is likely due to a combination of degeneration of the retina and increased stimulus thresholds in *rd*, which broadens the activated area of the retina.

Translational Relevance: Loss of retinotopy is evident in *rd* rats. If a similar loss of retinotopy is present in humans, retinal prostheses design must include flexibility to account for patient specific variability.

Introduction

The two most common outer retinal degenerative diseases are age-related macular degeneration (AMD) and retinitis pigmentosa (RP). RP is a general term for a disparate group of inherited diseases with over 200 genetic mutations that have been identified so far. The etiology of AMD is multifactorial[1,2] and includes genetic mutations in photoreceptors and accumulation of drusen. Age, smoking, race (more common among Caucasians than among African-Americans or Hispanics/Latinos), and family history are the main risk factors for AMD. AMD is more prevalent, but RP is more severe and both are characterized by progressive loss of photoreceptors. The photoreceptor loss in AMD and RP can lead to complete blindness and profound disability. It is estimated that approximately 15 million people suffer from vision loss due to these diseases worldwide, and these numbers are expected to rise as the population ages.

The societal impact of outer retinal degenerative disorders is tremendous. These disorders are one of the leading causes of adult-onset blindness. Studies from multiple countries[3,4] of patients with AMD has shown that the disease has a significant emotional and functional impact on patients, providers, and society

overall. In the United States, there are approximately 700,000 new AMD patients each year,[5,6] 10% of who will become legally blind. As the United States population ages, it is estimated[7] that more elderly persons will become blind from AMD than from glaucoma and diabetic retinopathy combined. A value-based analysis[8] of the societal burden of AMD estimates the yearly cost of the disease borne by the United States economy to be $30 billion. Because these studies are restricted to AMD, they underestimate the societal impact of the full spectrum of outer retinal degenerative diseases. While RP has a lower incidence than AMD, affecting approximately one in 2000 individuals worldwide,[9] the individual impact is more devastating and costlier due to the earlier onset and greater severity of RP compared with AMD.

There is currently no known cure for vision loss caused by outer retinal degeneration. Postmortem histologic analysis of retinal tissue in RP and AMD patients has given us valuable insight. Even when photoreceptor cell loss is virtually complete, other cells in the retina generally survive,[10] enough to be activated[11] by electrical stimulus. This finding provided the impetus for using implantable electronic retinal prostheses to provide functional vision for patients with blindness due to photoreceptor degeneration. Photoreceptor degeneration has been shown[12] to lead to extensive remodeling in the inner retina. Electronic retinal prostheses electrically stimulate surviving neurons and circuitry in the inner retina and represent an emerging technology[13] in the treatment of such diseases.

There has been limited previous research in characterizing in vivo visual cortex electrophysiology response elicited by epiretinal electrical stimulation of retina. Published results have been limited to experiments performed on three anesthetized cats that primarily investigated safety and surgical technique[14] of stimulating electrode array implantation. Two studies have compared cortical responses elicited by photovoltaic subretinal prostheses with visual-evoked potentials[15,16] in normally sighted and blind rats. More recently, intrinsic optical imaging was used to study the visual cortex response elicited by light stimulus versus electrical stimulus applied to subretinal electrode arrays in normally sighted rats.[17]

Rat models of retinal degeneration have greatly improved the understanding of the pathophysiology[17] of photoreceptor degenerative diseases. Rats have also been used to characterize retinotopic maps of the visual cortex activity[18] in response to light stimulus and electrical stimulus applied subretinally in normally sighted rats.[17] In this paper, we characterize electrophysiologic response in the visual cortex of healthy Long Evans rats and retinal degenerate (*rd*) S334ter line 3 rats elicited by electrical stimulation of the retina. Electrophysiology recording using microelectrodes in the visual cortex provides a functional readout in the visual system of the effect of electrically stimulating the retina. The human (and rat) visual cortex has an orderly arrangement of visual field processing, termed retinotopy. This retinotopic organization represents specificity in the spatial organization of connections in the various layers of the visual system with respect to the visual field, and is an important element of functional vision. Maintenance of retinotopy after photoreceptor loss is unclear. One of the overarching goals in the development of retinal prostheses is to provide functional vision for patients suffering from photoreceptor degeneration. Because retinotopy is a fundamental aspect of functional vision, our research aims to investigate the nature of cortical retinotopy elicited by the electrical stimulation of the retina in normally sighted and blind rats. This paper presents the first work in the study of visual cortex retinotopy in response to epiretinal electrical stimulation of the healthy versus *rd* retina. While the anatomic changes in the retina in response to photoreceptor degeneration are well studied, the effect on visual cortex neurons has not been studied as extensively. We present preliminary comparison of anatomic differences in the visual cortex neurons between normally sighted and blind rats using the Golgi stain and comparing spine density.

Materials and Methods

Animals

Healthy Long Evans (postnatal day P90–P120, $n = 9$) rats and S334ter line 3 rats with retinal degeneration (*rd*) (P120–P300, $n = 11$) were used for cortical response mapping of electrical stimulation of retina in four quadrants of the retina. The weight of the *rd* rats ranged from 228 to 278 g (mean 256 g with standard deviation of 21.1 g). The weight of the *rd* rats ranged from 270 to 321 g (mean 298 g with standard deviation of 19.3 g). The retinal degenerate rats were bred in the USC animal care facilities by mating homozygous S334ter line 3 rats with Long Evans rats (Envigo, Hayward, CA). The homozygous S334ter line 3 rats for breeding were obtained from the Rat Resource Research Center of the University of

Missouri. Because the mutation is dominant, all offspring had one copy of the mutated gene, and all experiments were conducted on these offspring. The rats were housed in covered cages and fed a standard rodent diet and water ad libitum while kept on a 12:12-hour light-dark cycle in the animal facility. All experimental procedures were approved by the Institutional Animal Care and Use Committee (IACUC) at the University of Southern California and adhered to the ARVO Statement for the Use of Animals in Ophthalmic and Visual Research.

Surgical Procedures

All surgeries were performed under general anesthesia. An intramuscular injection of a cocktail of ketamine (100 mg/kg; Ketaset, Fort Dodge Animal Health, Fort Dodge, IA) and xylazine (100 mg/kg; X-Ject SA, Butler, Dublin, OH) was used to induce anesthesia. Sevoflurane (0.5%–1% in 100% oxygen) administered through a mask attached to the stereotaxic bench was used to maintain anesthesia throughout the entire experiment. The rat's vital signs were monitored and the body temperature was maintained at 37°C with a self-regulated heating blanket (model 50-7053-F; Harvard Apparatus, Holliston, MA). Animals were euthanized after the experiment using an overdose of pentobarbital (0.5 mL; Euthasol; Virbac US, Fort Worth, TX) intracardiac injection.

Craniotomy and Recording Electrodes

The anesthetized rat was affixed to a stereotaxic bench using ear bars (Model 900; David Kopf Instruments, Tujunga, CA). The skull was exposed and a craniotomy was performed on the right side (caudal-medial corner: ~5 mm caudal and ~5 mm lateral to lambda) using a hand-held drill. A three electrode (recording, reference, ground) recording system was used to capture electrophysiologic signals in the visual cortex elicited by electrical stimulation of the retina. Epoxy-coated tungsten microelectrodes (10 MΩ impedance; FHC, Bowdoin, ME) were used for electrophysiology recording from the visual cortex. The recording electrode was affixed to an electrode holder that was attached to the stereotaxic bench. A digital readout provided the electrode holder's three-dimensional position in space with micrometer accuracy. The rat skull landmark lambda where the posterior suture lines meet was used as the origin for recording electrode positioning. The visual cortex in rat brains generally spans a depth of 1.5 mm from the cortical surface,[20] and the recording electrode was positioned midway within the visual cortex at a depth of 700 to 750 μm from the cortical surface on the right side. The reference electrode was placed in the anterior cortex at a similar depth, and the ground electrode was connected to a bone screw implanted into the left side of the skull.

Stimulation Electrodes

A flat-tipped concentric bipolar platinum/iridium (Pt/Ir) electrode (model CBDFG74; FHC, Bowdoin, ME) was used to electrically stimulate the rat retina. The inner pole diameter was 75 μm and the outer pole diameter was 300 μm. For all the experiments with *rd* rats, the stimulation electrode tip was coated to effectively have a high surface area of charge injection, allowing the electrode to safely deliver higher levels of stimulus to the retina. High surface area Pt/Ir thin-film coating was formed on the standard Pt/Ir microelectrode using electrodepostion methods developed[21] in our laboratory. The stimulation electrode was used in a monopolar configuration with either the inner pole or outer pole used for stimulating the retina. The return electrode was a large surface area platinum needle inserted in the skin adjacent to the nose. To insert the stimulation electrode, the left eye of the rat was first dilated with a few drops each of 1% tropicamide (Tropicacyl; Akorn, Buffalo Grove, IL) and 2.5% phenylephrine (AK-Dilate; Akorn). A small piece of a latex surgical glove was used to proptose the eye. A glass coverslip covered with an ophthalmic demulcent gel (Akorn, Goniosol, Gonak) pressed to the cornea allowed focused viewing of the fundus through an operating microscope. The stimulation electrode was inserted through a scleral incision near the limbus. The distance of the stimulation electrode from the retina was monitored indirectly by measuring the electrochemical impedance[22] with a potentiostat (Gamry Instruments, Warminster, PA), an established method in our laboratory that has been previously validated using optical coherence tomography images of the electrode—retina interface. For this study, the electrode was placed 50 to 100 μm from the epiretinal surface, based on nominally having an 8-kΩ electrode impedance measured at 100 kHz.

Electrical Stimulation of the Retina

Charge balanced biphasic stimulus current pulses of amplitude ranging from 30 to 1000 μA and 0.5 ms pulse width were delivered to the retina at the rate of 1 Hz. The cathodic first biphasic pulses had an

interphase interval between the cathodic and anodic phases of 100 μs. The cathodic first biphasic pulse configuration for retinal stimulation was used for our study as it is the standard pulse waveform used in previous epiretinal stimulation studies and in commercial retinal prostheses that are currently in use.[13] We used suprathreshold stimulus amplitudes for the experiments in this study as such amplitudes are used in retinal prostheses clinically with the aim of providing vision with adequate brightness to patients. An initial threshold estimate was made (described in the next section, Electrically Evoked Response [EER] Acquisition) during the experiment to set stimulus levels to be 3.3 times the threshold for cortical mapping for healthy rats and 2 to 3 times the threshold for *rd* rats. The stimulus pulses were generated by a current to voltage converter (model 2200; A-M Systems, Sequim, WA), driven by a voltage pulse from a programmable analog output card (DataWave Technologies, Berthoud, CO) on a personal computer running Datawave's software. An oscilloscope was used to monitor output current (across a sense resistor) to ensure that stimulator compliance voltage did not limit or distort the output current.

Electrically Evoked Responses (EER) Acquisition

EERs in the primary visual cortex elicited by electrical stimulation of the retina were acquired using recording microelectrodes. During the procedures described below, the recording electrode was moved in a grid pattern with a pitch of 250 μm, generally starting in the middle of the visual cortex or in the middle of the expected cortical area of response for light stimulus.[19] Not all grid points could be recorded because blood vessels on the cortical surface interfered. In this case, the location was skipped or a point nearby was used. To begin each recording session, threshold was estimated in a two-step process. First, EERs were recorded at multiple cortical locations using a range of stimulus settings that typically evoke minimal response (i.e., near threshold). At the cortical area that appeared (by visual inspection) to produce the most robust EER, the stimulus amplitude was lowered until EERs were observed approximately 50% of the time. This amplitude was deemed the threshold stimulus. A rapid threshold estimate was needed because maintaining the stimulating electrode in the eye for more than 2 hours was challenging (due to eye fluid leakage). Once a threshold estimate was obtained, cortical response maps were obtained by setting the stimulus amplitude level to 2 to 3 times the threshold and moving the recording electrode in a grid pattern as described above. At a subset of cortical sites, stimulus amplitude was swept from below threshold to approximately 5 times threshold and EER was recorded to characterize dose—response relationship of EER strength with respect to stimulus amplitude. The EER was amplified with a gain of 2000 and band-pass filtered (150 Hz to 8 kHz) prior to sampling at 20 kHz. For each stimulus condition, the EER was averaged over 50 stimulus pulses. Figure 1 illustrates an overview of the experimental setup and representative EER traces.

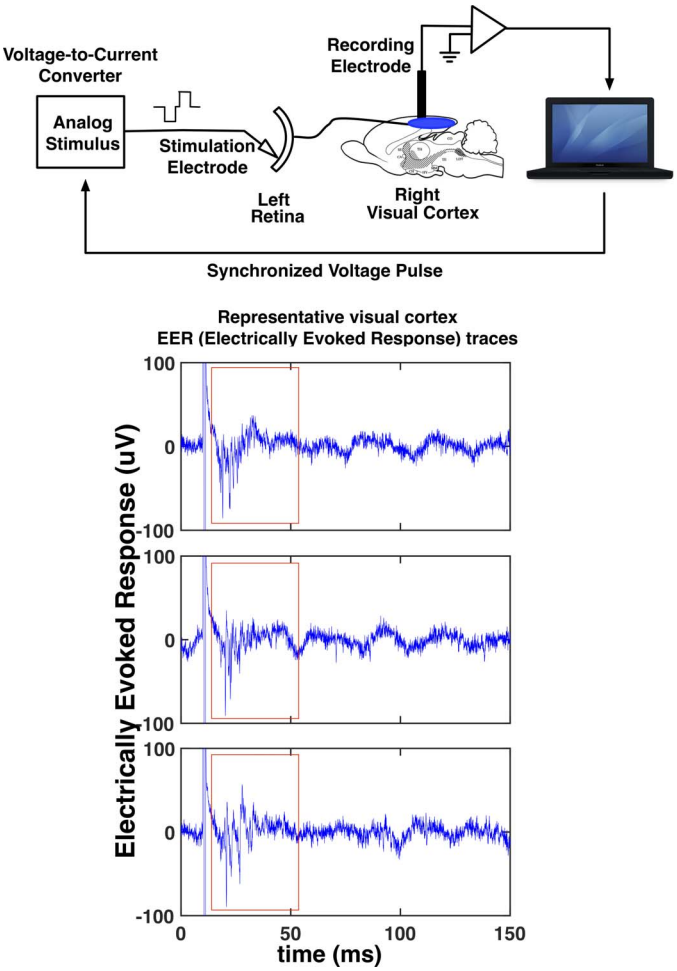

Figure 1. Electrophysiology experiment setup schematic (*above*), shown with representative visual cortex recordings elicited by electrical stimulation of the retina (*below*). The stimulus pulse was delivered at 10 ms. The *red boxes* show the time window for EER strength calculation.

EER Analysis

Off-line filtering (done after the experiment) included digital filtering to remove high frequency and 60-Hz noise. High-frequency noise above 10 kHz was filtered using a software filter built into the data acquisition software (SciWorks; DataWave Technologies, Berthoud, CO). The digital bandstop filter with a 60 Hz center frequency was implemented in MATLAB (MathWorks, Natick, NY) using a least squares finite impulse response (FIR) filter with a 20 kHz sampling frequency and a minimum order to generate a bandstop range of ±2 Hz from the center frequency. EERs were recorded at multiple sites in the visual cortex of each rat, and each cortical location's stereotaxic co-ordinates (relative to lambda) were recorded. The root mean square (rms) value of the EER (signal) was compared with the rms value of baseline noise (noise), recorded before stimulus, to calculate signal-to-noise ratios (SNR) for each stimulus condition. EER strength values were obtained by computing the integral of the mean square of recorded signal from 3 to 40 ms poststimulus. This range captured the entire EER while avoiding the stimulus artifact, which was not present beyond 2 ms in most cases. When higher currents were used, stimulus artifact extended to 5 ms, requiring subtraction of the stimulus artifact prior to integrating the EER. Following published methods,[23] artifact for no-responsive trials was subtracted from responsive trials. We defined EERs to be detectable at a given cortical location if the SNR was greater than 10 dB. The cortical location with highest SNR of the EER for a given retinal stimulation electrode placement was marked as the maximal response location for the cortical response maps (see Results).

Golgi Staining

Normal Long Evans (P200–P300, $n = 6$) rats and S334ter line 3 rats with retinal degeneration (P250–P300, $n = 6$) were also used for comparing the neuroanatomy of the visual cortex. These rats were not used for electrophysiologic experiments. The rat brains were processed using the Golgi stain. The rat was deeply anesthetized using the ketamine/xylazine as described above, then euthanized with an overdose of sodium pentobarbitol (0.5 mL of Euthasol) was injected intracardiac. Golgi-Cox staining (PK401 Rapid GolgiStain Kit; FD NeuroTechnologies, Ellicott City, MD) was used to visualize neurons in the visual cortex. The brains were dissected immediately after euthanasia and the tissue was impregnated for 2 to 3 weeks in the dark in a Golgi-Cox solution containing mercuric chloride, potassium dichromate, and potassium chromate with the solution replaced after the first 24 hours. The brain tissue was then moved to a cryoprotection solution for 48 to 72 hours. They were then sectioned coronally into 100- to 150-μm sections on a vibratome. The sections were mounted on gelatin-coated slides and dried overnight. The slides were developed the next day using the Rapid Golgi Stain kit developing solution. Briefly, the slides were rinsed in distilled water twice for 4 minutes each and placed in a developing solution for 10 minutes. The slides were then rinsed and dehydrated in 50%, 70%, 95%, and pure alcohol for 4 minutes each and cleared in Xylene 3 times for 4 minutes each. The slides were then cover-slipped with Permount and stored in the dark until morphologic analysis was performed.

Morphologic Analysis of Visual Cortex Neurons

In the Golgi-stained rat brain sections, neurons in the visual cortex with somas lying approximately 700 to 900 μm below the cortical surface were analyzed as that region corresponded to the placement of recording electrodes for electrophysiology experiments.

In previous studies of dendritic spines in the visual cortex of rats, it has been found[24] that most of the excitatory synapses are located in a roughly spherical volume centered about the soma that contains the basal and proximal majority of oblique dendrites. Accordingly, basal and oblique dendrites were sampled at different visual cortex locations across the sampled brain sections from all the rats.

Dendritic spine density was calculated by dividing a neuron's traced dendritic length by the spine count total along the traced dendrite, and expressed as number of dendrites per 10 μm length of dendrite. Dendritic length was obtained by tracing dendrites starting about 30 to 40 μm away from the soma until the dendrite was cut off focus or near the terminus where the number of spines tapers off. Spine counts were obtained by manually counting dendritic spines along the traced dendrites. All morphologic data were collected at ×60 and ×83 magnification with an Olympus Corporation BX50 microscope (Shinjuku, Tokyo, Japan) using a QImaging QIClick camera (Surrey, British Columbia, Canada) to acquire images that were analyzed using ImageJ software (http://imagej.nih.gov/ij/; provided in the public domain by

the National Institutes of Health, Bethesda, MD, USA). GraphPad QuickCalcs software (La Jolla, CA) was used for statistical analysis of dendritic spine density. A student's *t*-test was used to compare the mean dendritic spine density of the visual cortex neurons between normal and blind rats. A *P* value of less than 0.05 is considered as a statistically significant difference.

Results

Cortical Electrophysiology Response Characteristics

EERs generally show a dose response relationship in both normal and *rd* rats. Figure 2 shows representative plots of EER at one cortical location in a healthy rat for increasing stimulus amplitudes from 25 to 100 μA. EER strength was measured at 14 cortical locations in four healthy Long Evans rats as the stimulus amplitude was varied from 30 to 100 μA. A dose-response relationship was observed in the cortical EER strength with respect to stimulus current delivered to the retina. Some cortical locations ($n = 5$) showed monotonic behavior and some locations ($n = 9$) showed peak EER strength at intermediate current. EER strength was also measured at 15 cortical locations in four *rd* S334ter line 3 rats as the stimulus amplitude was varied from 100 to 1000 μA. Just as in the healthy rats, a dose response relationship was observed in the cortical EER strength in *rd* rats with respect to stimulus current delivered to the retina. Once again, some cortical locations ($n = 4$) showed monotonic behavior, and some cortical locations ($n = 11$) showed peak EER strength at intermediate current in *rd* rats. The dose-response curves for both the healthy and *rd* rats are shown in Supplementary Figures S1 to S4.

As described in the methods, an initial threshold estimate was made during the experiment to set stimulus levels used during mapping. The threshold estimates in healthy rats ranged from 10 to 15 nC of charge per stimulus pulse for 0.5 ms wide pulses. For the study of cortical retinotopy, stimulus amplitude for normal rats were set to 100 μA, which was 3.3 times typical threshold. The thresholds in *rd* rats were higher and ranged from 100 to 200 nC of charge per stimulus pulse for 0.5 ms wide pulses. For the study of cortical retinotopy, stimulus amplitude for *rd* rats were set between 400 to 600 μA, which were 2 to 3 times the threshold. The use of high surface area Pt/Ir thin film[25] at the tip of the stimulation electrode was necessary to be able to deliver charge densities as high as 10 mC/cm^2, though this was not a typical stimulus level. No bubbles were observed in the vitreous at the highest charge densities used for stimulation over a few hours during which data were collected. The use of high charge density pulses intermittently may be tolerable, although such levels used for an extended time are likely to be unsafe, regardless of which electrode material is used.

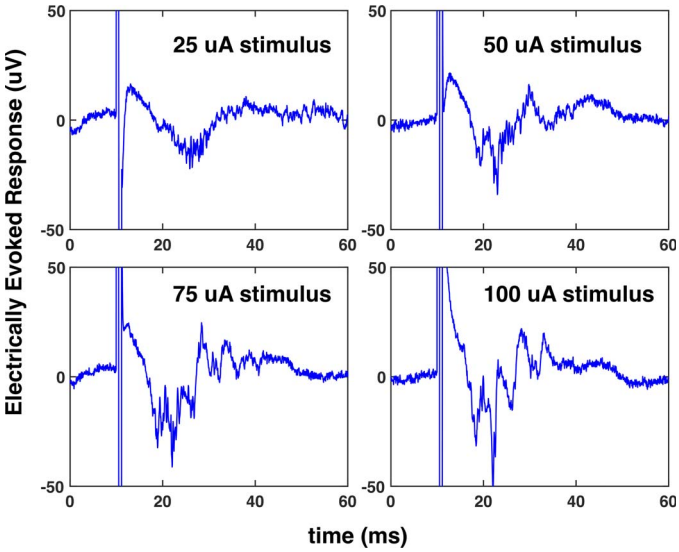

Figure 2. Representative EER traces in the visual cortex of a normal rat for increasing stimulus current amplitude delivered to the retina. Each trace is averaged over 50 trials. Stimulus pulse is delivered at 10 ms for each stimulus amplitude.

Retinotopy of Cortical Activity in Normal Rats

Cortical activity maps for nine healthy Long Evans rats were obtained with the stimulation electrode placed in four quadrants around the optic disk: ventral temporal, ventral nasal, dorsal nasal, and dorsal temporal retina. The stimulus amplitude used for generating cortical activity maps in all the healthy rats was 100 μA (see Methods). Figure 3 shows the orientation of the four retinal quadrants where the stimulation electrode was placed. Figure 4 shows representative cortical response maps for each of the four retinal quadrants that were stimulated. It should be noted that our cortical activity maps use the anatomic landmark of the posterior cranial sutures' junction as the origin (for stereotactic mapping). This is in contrast to the anterior cranial sutures' junction used as the origin in previously published maps of cortical activity in response to light stimulation of the

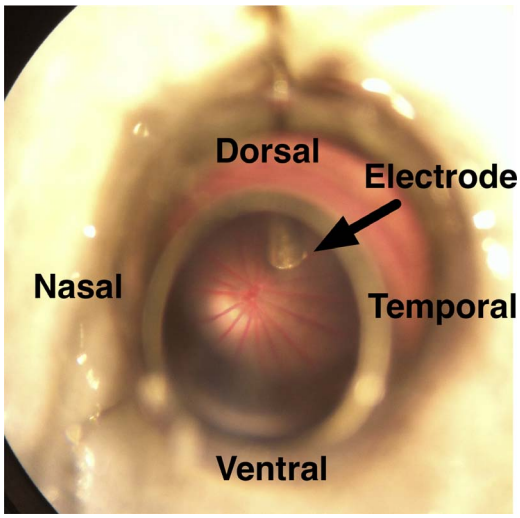

Figure 3. Representative image of the left eye of a normal rat seen through an operating microscope with a coverslip coated with Gonak ophthalmic demuclent gel gently pressed to the cornea. The tip of the stimulation electrode marked by the *arrow* and is placed in one of four retinal quadrants for each cortical recording session.

rat retina.[19] This results in an approximately 7.5 mm difference in the anterior–posterior coordinates (y axis) of the cortical response maps. In the results below, we subtract 7.5 mm from the y-axis bounds for each region reported in a previously published light-stimulation study[19] to allow for easier comparison between the two studies.

In four rats where the stimulation electrode was placed in the ventral temporal quadrant of the retina, detectable EERs were recorded 3.25 to 4 mm lateral to lambda and 0.75 mm anterior to 0.5 mm posterior to lambda. Light stimulus of ventral temporal retina (dorsal-nasal visual field) has been shown to evoke cortical activity in the region 3 to 5 mm lateral to lambda and 2 mm anterior to 0.5 mm posterior to lambda.[19]

In three rats where the stimulation electrode was placed in the ventral nasal quadrant of the retina, detectable EERs were measured 1.5 to 3.2 mm lateral to lambda and 0.5 mm anterior to 0.5 mm posterior to lambda. Light stimulus of ventral nasal retina (dorsal temporal visual field) has been shown to evoke cortical activity in the region 2 to 3.5 mm lateral to lambda and 1 mm anterior to 1.5 mm posterior to lambda.[19]

In one rat where the stimulation electrode was placed in the dorsal-nasal quadrant of the retina, detectable EERs were measured 1.75 to 2.25 mm lateral to lambda and 0 mm to 0.75 mm anterior to lambda. Light stimulus of dorsal-nasal retina (ventral temporal visual field) has been shown to evoke cortical activity in the region 1.25 to 2.5 mm lateral to lambda and 1.25 mm anterior to 0.5 mm posterior to lambda.[19]

Inserting the stimulation electrode in the dorsal half of the retina is challenging. The retina is very sensitive to mechanical pressure and the incision for the electrode insertion followed by the placement of the electrode frequently caused retinal detachment in the dorsal retina, limiting the number of cortical maps we could obtain for dorsal retinal stimulation. A partial activity map was obtained in one healthy rat where the stimulation electrode was placed in the dorsal-temporal quadrant of the retina. Detectable EERs were recorded 1.75 to 2 mm lateral to lambda and 1.5 to 2.5 mm anterior to lambda. Light stimulus of dorsal-temporal retina (ventral-nasal visual field) has been shown to evoke cortical activity in the region 1.5 to 4 mm lateral to lambda and 1.5 to 3.5 mm anterior to lambda.[19]

A composite activity map of visual cortex responses elicited by electrical stimulation of the healthy rat retina in the four quadrants is shown in Figure 5. Each dot on the composite map represents a cortical location where EERs were detected in response to suprathreshold electrical stimulation of the healthy retina across nine rats, with the four different colors representing the four different quadrants of the retina that were stimulated. The cortical locations mapped are color coded with the location of the stimulation electrode: blue for ventral temporal retina, red for ventral nasal retina, orange for dorsal nasal retina, and green for dorsal temporal retina. The regions of cortical activity for the different regions of retinal stimulation are clearly delineated.

Retinotopy of Cortical Activity in *rd* Rats

Cortical activity maps for eleven *rd* rats were obtained. All of the *rd* rats required higher amplitude stimulation of the retina to show cortical activity, ranging from 400 to 600 μA of current per pulse. All of the stimulus amplitudes used for cortical activity mapping in *rd* rats were 2 to 3 times the threshold that was measured at the start of the experiment, as described in the Methods section above. A pulse width of 0.5 ms was used for the cathodic and anodic phases of the biphasic stimulus pulse, with an interphase interval of 0.1 ms. Figure 6 shows representative cortical response maps for each of the four retinal quadrants that were stimulated in *rd* rats,

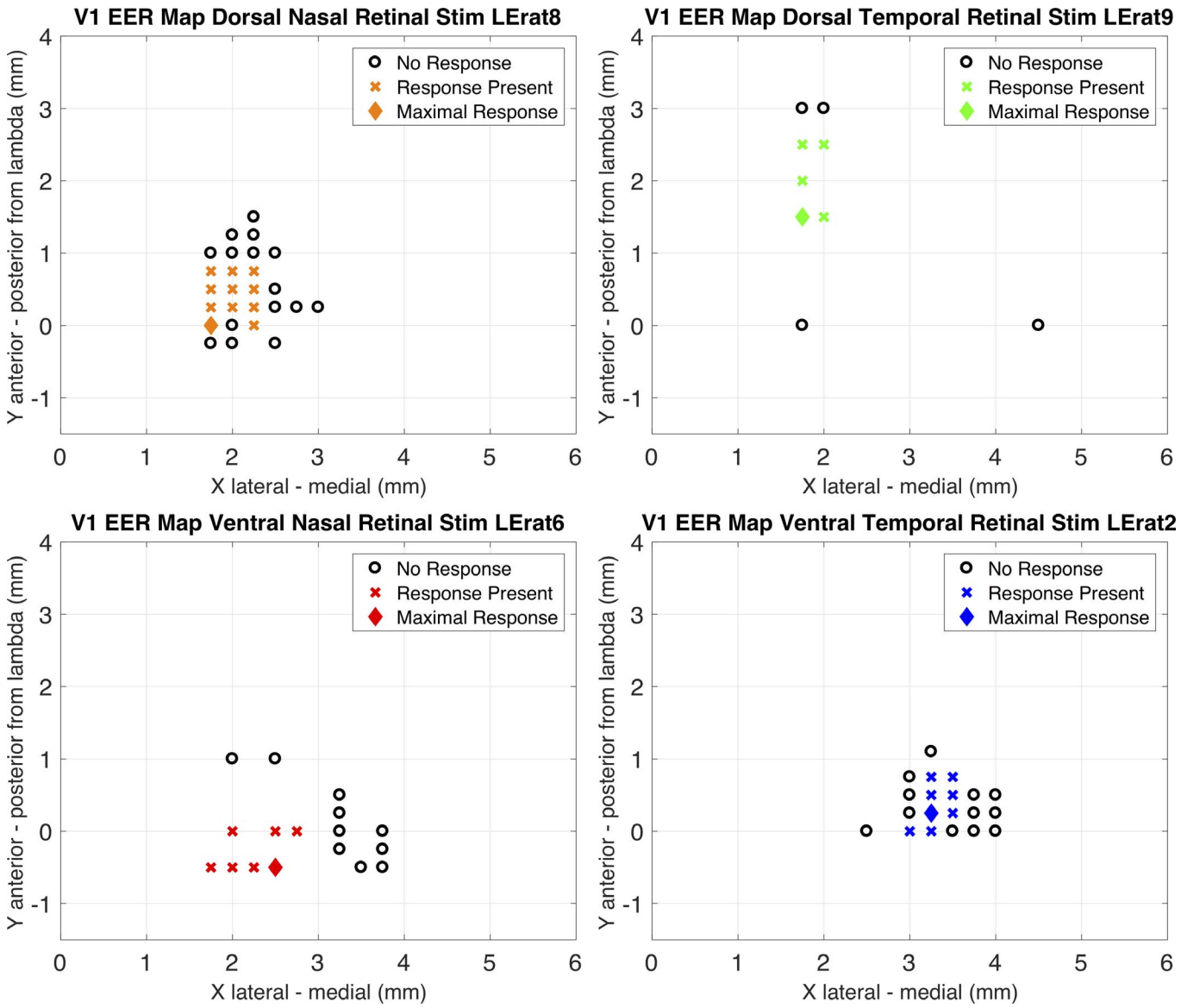

Figure 4. Representative visual cortical response maps for the four retinal quadrants where the stimulation electrode was placed in healthy rats. Stimulus current amplitude of 100 μA, which was 3.3 times the typical threshold was used for all maps. The maps show all the cortical locations sampled for each rat and indicate sites of maximal, submaximal, and no response.

and the stimulus amplitude used for each of the maps is indicated in the figure.

In three *rd* rats where the stimulation electrode was placed in the ventral temporal quadrant of the retina with stimulus amplitudes of 450, 600, 600 μA, detectable EERs were recorded 2 to 4.25 mm lateral to lambda and 2.5 mm anterior to 1 mm posterior to lambda. All three *rd* rats with ventral temporal retinal stimulation show cortical activity outside the region of cortical activity seen for light stimulus.

In three *rd* rats where the stimulation electrode was placed in the ventral nasal quadrant of the retina with stimulus amplitudes of 450, 600, 600 μA, detectable EERs were measured 2 to 3.75 mm lateral to lambda and 1 mm anterior to 0.75 mm posterior to lambda. In general, all three rats with ventral nasal retinal stimulation do show cortical activity in the same cortical region as seen in light-stimulus experiments. However, the borders of activity do not seem as well defined as seen in healthy rats.

In four *rd* rats where the stimulation electrode was placed in the dorsal nasal quadrant of the retina with stimulus amplitudes of 400, 400, 450, 450 μA, detectable EERs were measured 1.5 to 4 mm lateral

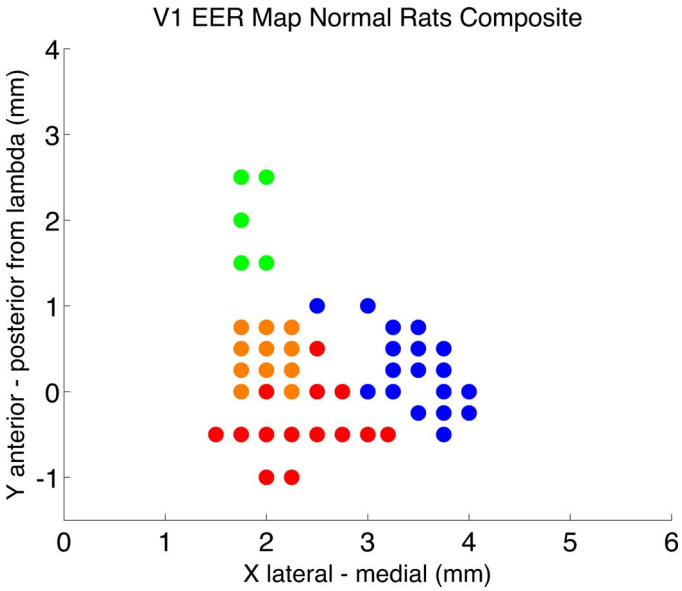

Figure 5. A composite map of cortical activity in nine Long Evans healthy rats in response to epiretinal electrical stimulation of the retina. The four colors represent the four quadrants of the retina where the stimulation electrode was placed: *blue* for ventral temporal retina, *red* for ventral nasal retina, *orange* for dorsal nasal retina, and *green* for dorsal temporal retina. Each *dot* on this composite map represents a cortical location where electrophysiology activity was recorded in response to electrical stimulation of the retina, with the four different colors representing the four different quadrants of the retina that were stimulated.

to lambda and 1 mm anterior to 0.5 mm posterior to lambda. Three of the four *rd* rats with dorsal nasal retinal stimulation show activity outside the region of cortical activity seen for light stimulus of dorsal nasal retina. Additionally, in two *rd* rats, the boundaries of activity were less defined with locations of response and no response intermingled with each other.

In one *rd* rat where the stimulation electrode was placed in the dorsal temporal quadrant of the retina with stimulus amplitude of 600 μA, detectable EERs were measured 2.25 to 3.5 mm lateral to lambda and 2 mm anterior to 0.75 mm posterior to lambda. This *rd* rat with dorsal-temporal retinal stimulation shows cortical activity outside the region of cortical activity seen for light stimulus of dorsal temporal retina.

A composite activity map of visual cortex responses elicited by electrical stimulation of *rd* rat retina in the four quadrants is shown in Figure 7. Each dot on the composite map represents a cortical location where EERs were detected in response to suprathreshold electrical stimulation of the *rd* retina across 11 rats, with the four different colors representing the four different quadrants of the retina that were stimulated. It can be seen that there is a large overlap in the regions of cortical activity for the different quadrants of retina that were stimulated, and the retinotopic organization in the visual cortex seen for normally sighted rats is disrupted in blind rats.

Spontaneous Activity in the Visual Cortex of *rd* Rats

Visual cortex recordings without retinal stimulation were performed at $n = 29$ cortical locations in seven normal Long Evans rats and at $n = 78$ cortical locations in 18 S334ter line 3 *rd* rats. The recordings spanned a time window of 0.5 seconds with 50 trials at each cortical recording location. The offset in the recorded signal was removed by subtracting the mean of the recorded signal over each 0.5-second time window. The power at each cortical location was measured by rectifying and integrating the signal over the 0.5-second time window and averaged over the 50 trials.

Figure 8c shows a bar graph comparing the mean power in the visual cortex electrophysiology recordings with no retinal stimulus between healthy and *rd* rats. The error bars show standard deviation calculated from pooled variance across all the cortical locations and trials. A student's *t*-test shows that the power in the visual cortex recording of *rd* rats (mean 2.45, standard deviation 0.90, units μV^2*1e5) is more than in healthy rats (mean 1.80, standard deviation 0.12) and is statistically significant ($P = 0.0002$). Figures 8a and 8b show the distribution of the mean power measured in visual cortex electrophysiology recordings for healthy and *rd* rats, respectively, when no retinal stimulation was applied. The histograms show a shift to the right for the *rd* rats in comparison with healthy rats, indicating that there is more spontaneous activity in the visual cortex of *rd* rats in comparison with healthy rats.

Visual Cortex Dendritic Spine Density Comparison

A representative image of a rat brain section with the Golgi stain viewed at high magnification (×60) used for dendritic spine counting is shown in Figure 9.

Figure 10 shows a comparison of the spine density between the healthy and *rd* rats, expressed as the mean number of spines counted per 10-μm length of dendrite. The visual cortex neurons of *rd* rats shows an approximately 10% higher dendritic spine density than in the healthy rats, which is a small but statistically significant difference (student's *t*-test, $P = 0.043$). For the Long Evans rats, the mean number of spines per 10 μm of dendrite length was 2.78, with a

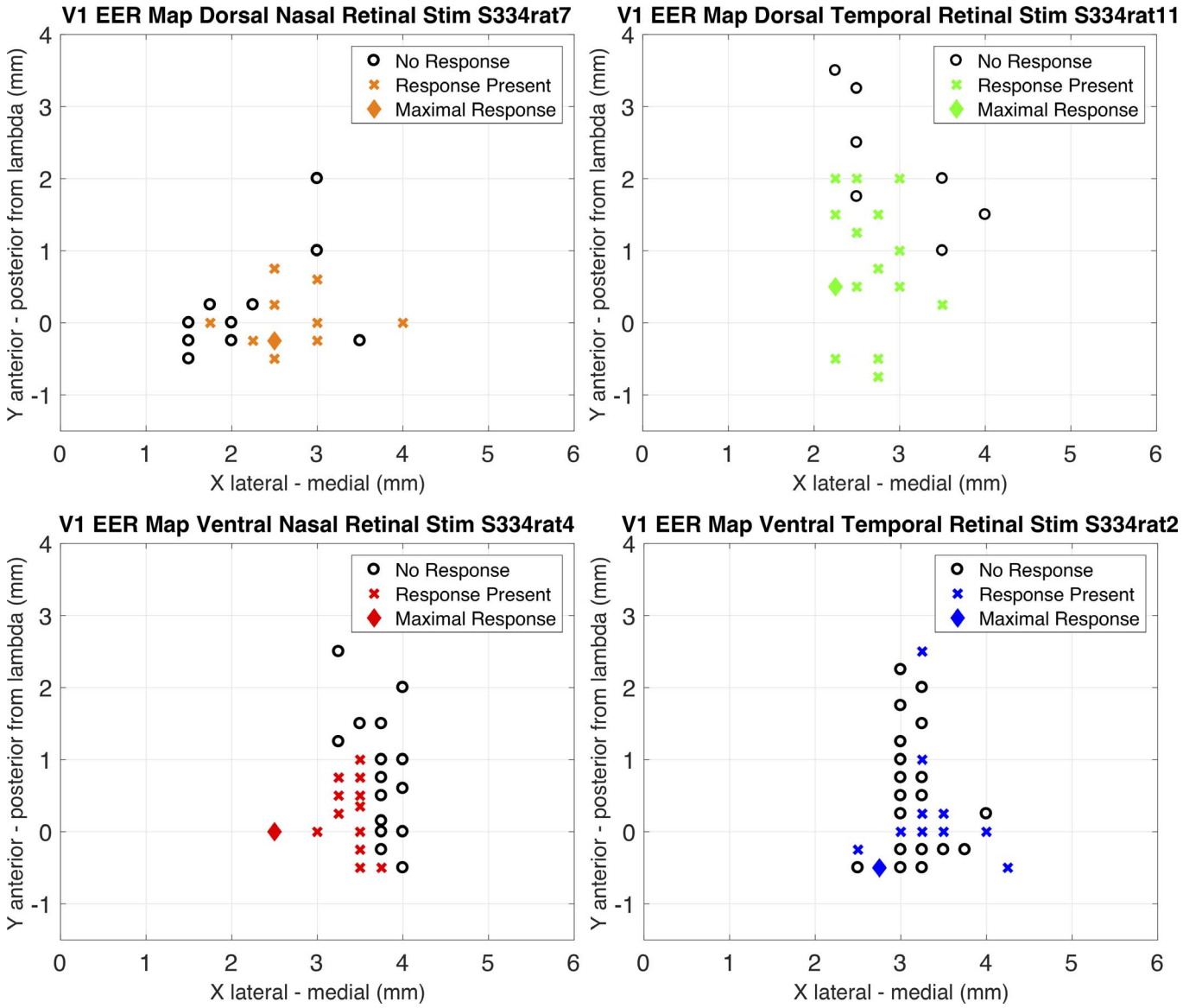

Figure 6. Representative visual cortical response maps for the four retinal quadrants where the stimulation electrode was placed in retinal degenerate rats. Stimulus current amplitude of 400 μA was used for the dorsal nasal retinal quadrant map and 600 μA was used for the ventral temporal, ventral nasal, and dorsal temporal retinal quadrant maps. These stimulus current levels were 2 to 3 times the threshold estimated at the start of each experiment. The maps show all the cortical locations sampled for each rat and indicate sites of maximal, submaximal, and no response.

standard deviation of 0.71 and a 95% confidence interval of 2.78 ± 0.183. For the S334 rats, the mean number of spines per 10 μm of dendrite length was 3.05, with a standard deviation of 0.70 and a 95% confidence interval of 3.05 ± 0.188.

Discussion

Our experiments with healthy rats show that epiretinal electrical stimulation applied to a specific quadrant of rat retina elicits retinotopic visual cortex activity in the same region where light stimulus generates cortical activity, for all four quadrants of the retina where the stimulation electrode was placed. The experiments with *rd* rats show that retinotopy is not preserved in the visual cortex of the blind rats in response to electrical stimulation of the diseased retina. There is a large overlap in the regions of cortical activity for the different quadrants of diseased retina that were stimulated. The maps for the *rd* rats show a loss of retinotopy and more overlap in the

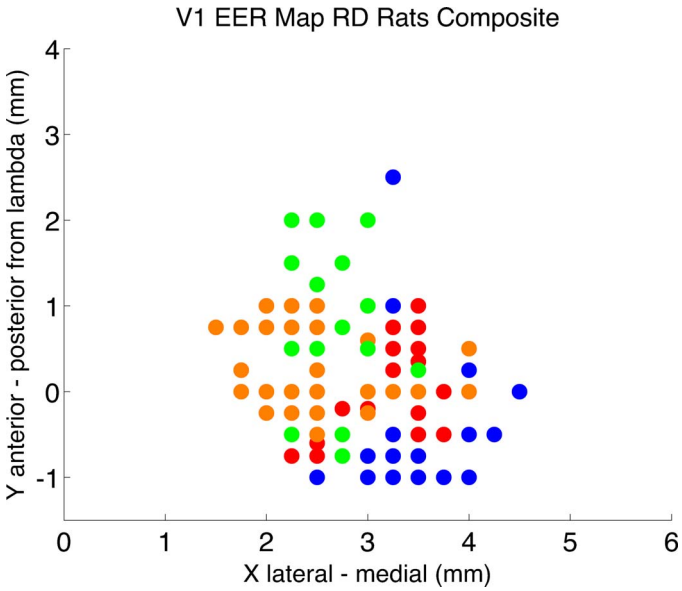

Figure 7. A composite map of cortical activity in eleven S334ter line 3 retinal degenerate rats in response to epiretinal electrical stimulation of the retina. The four colors represent the four quadrants of the retina where the stimulation electrode was placed: *blue* for ventral temporal retina, *red* for ventral nasal retina, *orange* for dorsal nasal retina, and *green* for dorsal temporal retina. Each *dot* on this composite map represents a cortical location where electrophysiology activity was recorded in response to electrical stimulation of the retina, with the four different colors representing the four different quadrants of the retina that were stimulated.

boundaries of the response areas. The changes seen in the cortical maps of activation for the *rd* rats could be due to the significantly higher stimulus currents used in the *rd* rats, due to remodeling of the visual cortical areas in response to loss of photoreceptors, or both. The *rd* rats had much higher thresholds for eliciting cortical responses, necessitating the higher stimulus currents for generating the cortical maps for the *rd* rats. To make a reasonable comparison between the cortical maps for the healthy versus *rd* rats, supra-threshold stimulus was used in both cases. Hence, our cortical map data are affected by the use of higher stimulus currents to stimulate the retina in *rd* rats. High-stimulus levels are sometimes noted in clinical studies, making these results important toward understanding why some patients with retinal implants do not perform as well as others. Other factors that should be considered when interpreting our results include uneven sample size for the four quadrants of retina stimulated, and incomplete maps caused by blood vessels and difficulties inherent in a two-electrode experiment. By bypassing blood vessels, the cortical recordings were not obtained in a perfect grid. It is possible that some of the optimal cortical response locations we report may be off by up to 150 μm.

A previously published study used intrinsic signal imaging (ISI) to measure activity in the visual cortex to generate cortical activity maps in response to light stimulus[19] in nondystrophic Royal College of Surgeons (RCS) rats. ISI is based on the principle that neuronal activity reduces the intensity of light reflected from brain and is a widely used technique[26] to study cortical plasticity. Providing a light stimulus to discrete areas of the rat's visual field induced a focal reduction in reflected light from the visual cortex indicating a localized increase in visual cortical activity. In addition, neighboring visual field stimulus locations evoked responses in neighboring visual cortical areas showing retinotopic organization in the visual cortex of normally sighted rats. Our study shows that this retinotopic organization is conserved in healthy rats for the artificial neural stimulus provided by electrical stimulation of the retina. The light stimulus–evoked cortical response maps showed variation in the absolute location of the retinotopic maps in stereotaxic coordinates between individual rats, but shared the same relative organization[19] of cortical activity. Our results in healthy rats show that epiretinal electrical stimulation applied to a specific quadrant of the rat retina elicits visual cortex activity in the same region where light stimulus generates activity. These results are consistent with another recently published study that compared cortical activity elicited by light stimulus versus electrical stimulation of subretinal electrodes[17] in normally sighted rats. Our experiments with *rd* rats show that there is a large overlap in the regions of cortical activity for the different quadrants of retina that were stimulated. Retinotopy is not as well preserved in the visual cortex of the blind rats in response to electrical stimulation of the diseased retina, which may be attributed to the significant remodeling seen in diseased retinas.[12] However, the *rd* rats required substantially higher stimulation amplitudes for cortical mapping due to the significantly higher thresholds required to stimulate the *rd* retina. While all of the cortical maps presented in this study were generated using stimulus amplitudes that were 2 to 3 times the measured threshold for both *rd* rats and 3.3 times the threshold for healthy rats, the higher current needed in *rd* rats may activate the axons of passage,[27] which would expand the cortical area activated and contribute to some of the disruption seen in the cortical activation maps of *rd* rats. Assuming that the rat

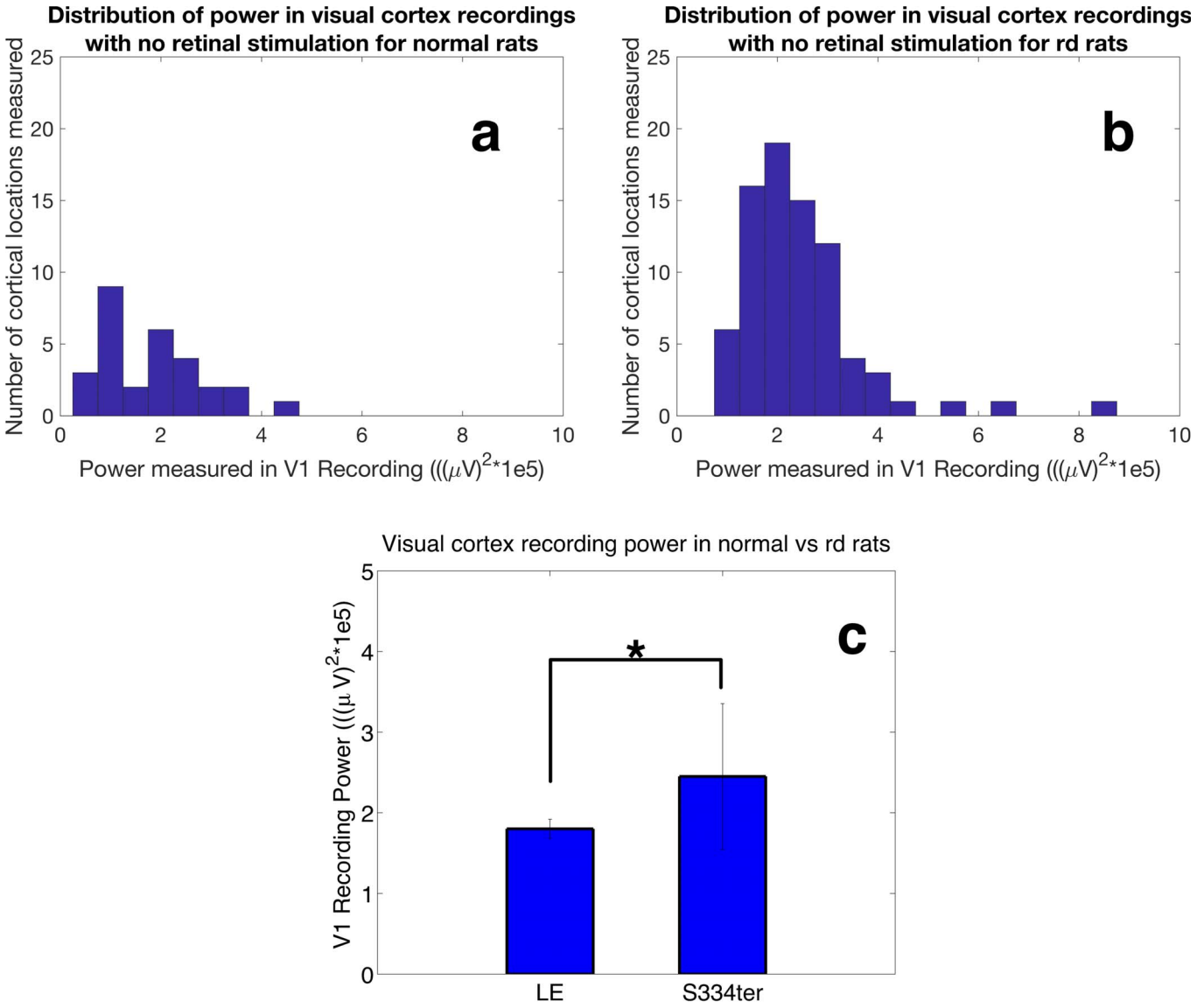

Figure 8. (a) Visual cortex spontaneous activity power histogram for normal rats distribution of the mean power in visual cortex electrophysiology recordings with no retinal stimulus at $n = 29$ cortical locations in seven normal rats. (b) V1 spontaneous activity power histogram for *rd* rats distribution of the mean power in visual cortex electrophysiology recordings with no retinal stimulus at $n = 78$ cortical locations in 18 *rd* rats. (c) Comparison of the mean power in visual cortex electrophysiology recordings of 500 ms duration with no retinal stimulus in $n = 29$ cortical locations in seven normal rats versus $n = 78$ cortical locations in 18 *rd* rats. The *error bars* indicate standard deviation; *statistical difference with $P = 0.0002$.

retina has 1° of visual angle for 60 μm of the retina,[28] a 75-μm electrode used to the stimulate the retina, if it created a 75-μm spot of activation, would activate 1.25° of visual angle in the rat. Based on the largest cortical magnification factor reported of 69 μm/°[19] for light stimulation of the retina, we would expect a cortical area of 86 μm to be activated. Because our area of activation is significantly larger, it is clear that we are activating a retinal area greater than the size of the electrode. This is not unexpected, given current spread that will occur due to even a small gap between the retina and electrode and due to the fact that we are stimulating well above threshold.

Cortical function degeneration has also been studied in the RCS rat model of retinal degeneration using intrinsic optical imaging.[19] Cortical response to various gratings and electrophysiology measurements in response to a pulse of broad-spectrum light were used to monitor the function of the visual cortex as the RCS rats aged. Prior to this study, behavioral

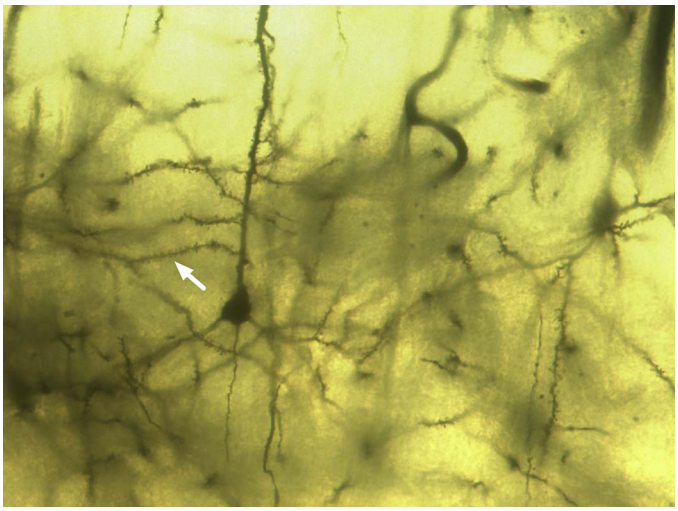

Figure 9. A representative coronal section of the visual cortex processed using the Golgi stain displayed at ×60 magnification and used for dendritic spine counting. The *white arrow* shows a typical basal dendrite used for spine counting.

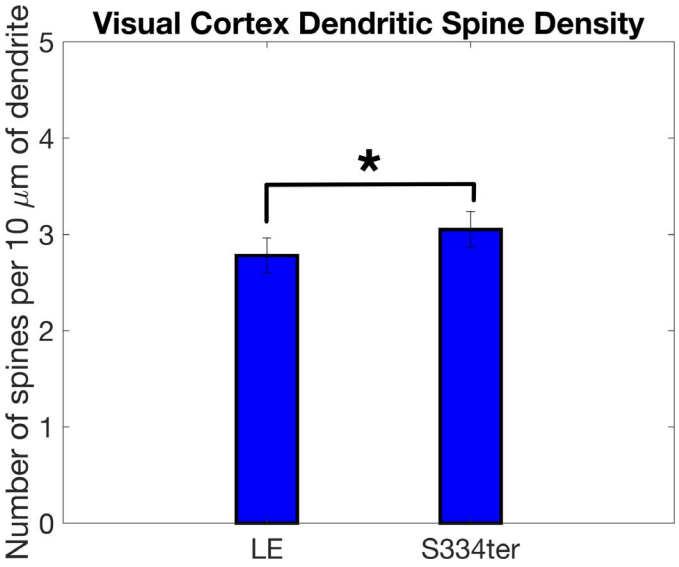

Figure 10. Comparison of dendritic spine density measured at 58 visual cortex locations in four Long Evans rats versus 56 visual cortex locations in three *rd* rats. The *rd* rats show a 10% higher spine density that is statistically significant; student's ***t***-test $P = 0.0433$. The ***error bars*** show 95% confidence intervals.

outputs of RCS rats led to the assumption that they develop normal visual function before degenerating as a result of disease in the photoreceptors. The measurements in this study showed significant deterioration of cortical processing of visual information starting around 4 weeks of age. So, changes in visual cortex function happen in this rat model before the development of the visual system in to its adult form is completed.[19]

Functional magnetic resonance imaging (fMRI) studies are increasingly being used to provide insight into visual cortical function changes due to outer retinal degeneration in human subjects. A recently published study[29] that analyzed visual cortex MRI data acquired from 13 RP patients with varying levels of peripheral retinal degeneration and 22 healthy control subjects showed functional remapping of the primary visual cortex as a function of visual impairment. A shift of central retinal representations to more peripheral locations was seen, with greater peripheral vision loss linked to larger remapping consistent with shifting of receptive fields into cortical regions with reduced retinal input. It is not clear whether this remapping is due to rapid cortical adaptation or long-term cortical reorganization, and studies with artificial scotomas in healthy subjects that match the visual field loss in patients may be needed to clarify the mechanism. In fMRI studies of patients with AMD, the results have been more disparate. Some studies[30,31] have found unresponsive or lower response visual cortical areas corresponding to the diseased central retina in AMD. Another study[32] used fMRI methods to explicitly evaluate visual cortical maps in patients with juvenile macular degeneration and adult AMD suffering from photoreceptor degeneration and compared the two sets with age-matched controls. They did not find evidence for large-scale remapping in the early visual cortical areas in adults with acquired retinal lesions, and found visual cortex activation no different than predictions based on normal retinotopic maps. They also found that this absence of cortical remapping was not dependent on the age at which the patients acquired retinal lesions in adulthood. Other studies[33] of AMD have found visual cortex reorganization when stimulating the peripheral retina. This study compared data from seven patients with varying levels of macular degeneration and six control subjects with no vision loss. They found that in five patients with complete loss of photoreceptors in the foveal region, there was large-scale reorganization in the visual cortex, while the two patients with foveal sparing did not show large-scale reorganization in visual processing in the cerebral cortex. A multicenter clinical trial[34,35] investigating electronic retinal prostheses has shown promising results for the treatment of patients with RP. The studies showed the implanted devices to be reliable and safe over years of use. In the vast majority of subjects, there was improvement in the

localization of high-contrast objects on a computer screen when using the prosthesis. A majority of subjects also showed improvement in detecting motion of a high-contrast bar when using the prosthesis. These are promising results, but a majority of the subjects did not show an improvement in their visual acuity measurement—the test commonly used clinically to grade functional vision performance. An objective understanding of how the visual system adapts to the chronic artificial input from an electronic retinal prosthesis is needed for improving the long-term performance of these prostheses. As can be seen from the disparate results from fMRI studies, limited information related to visual cortex plasticity can be gathered solely from human studies. There is a need to continue further animal studies to allow control of experimental variables (length of blindness, duration of treatment) as well as allow detailed anatomic analysis. The cortical maps of electrical stimulation of the retina from our study with acute retinal stimulation can be of use as a baseline to assess changes in cortical activation due to chronic stimulation and to investigate optimal strategies for intervention.

The dose-response curves were either monotonically increasing or exhibited a maximal response followed by a decline. The latter case may be due to a phenomenon known as upper threshold.[36,37] The monotonically increasing responses may not have yet reached upper threshold. More generally, the dose-response curves will be different due to experimental variables, including electrode positioning, (in *rd* animals) the condition of the retina, and the depth of anesthesia.

The thresholds for eliciting cortical activity in response to electrical stimulation of the retina in healthy rats ranged from 10 to 15 nC of charge per stimulus pulse for 0.5 ms wide pulses. Although the method used for determining threshold was a rough approximation based on observed traces, the range stated above is in the same range as seen in previous studies[38,39] of superior colliculus electrophysiology. Additionally, a dose-response characteristic was seen in the strength of the cortical responses elicited by increasing current amplitude of the retinal stimulation pulses. At some cortical locations, there was a monotonic increase in strength of the response, and some cortical locations showed maximal strength of response at intermediate current amplitudes. This could be attributed to the specifics of the visual system microcircuit that the stimulation electrode activated. This modulation of cortical response is consistent with the results from experiments[15,16,40] with subretinal photovoltaic stimulation, which showed that increasing the stimulus intensity (of the near-infrared light used to stimulate the photovoltaic cells) increases cortical response.

The thresholds for eliciting cortical activity in response to electrical stimulation of the retina in *rd* rats were significantly higher and ranged from 100 to 200 nC of charge per stimulus pulse for 0.5 ms wide pulses. The use of high surface area Pt/Ir thin film at the tip of the stimulation electrode was necessary to be able to deliver charge densities as high as 10 mC/cm^2.

Many previously published studies have shown that the thresholds for eliciting retinal and subcortical activity in response to electrical stimulation of the retina are higher in *rd* mice and rats when compared with wild-type controls. In *rd1* mice, in vitro electrophysiology experiments have shown thresholds to be 1.2 to 7.4 times higher[41–45] than in a healthy retina. Calcium imaging experiments using an in vitro rat retina preparation have shown thresholds to be up to 3 times higher for eliciting bipolar cell activity in *rd* rats when compared with healthy rats,[27] while retinal ganglion cell activity showed no change in stimulation threshold. Up to 4 times higher stimulation thresholds have been reported[37] for eliciting superior colliculus activity during in vivo electrophysiology experiments with *rd* rats when compared with healthy rats. It is reasonable to expect higher thresholds for in vivo experiments due to effects of anesthesia and due to the increased distance between the electrode and retina when compared with in vitro experiments with isolated retina.

The visual cortex recordings of *rd* rats also showed significantly more spontaneous activity than healthy rats when no retinal stimulation is applied. This is consistent with recently reported in vitro experiments of patch clamp recordings from diseased retina of *rd1* mouse retinal ganglion cells[46] and *rd10* mouse retinal ganglion cells that show greater spontaneous activity.[47] We did not observe periodic oscillations of activity, as has been observed in *rd* retina.[48] Another recently published study reported spontaneous neural activity in the primary visual cortex of S334ter *rd* rats,[49] in agreement with our results here.

While plasticity of dendritic spines is an area of robust research in neuroscience, there are few published studies that have investigated changes in dendritic spines due to blindness. In general, an increase in sensory experience increases the dendritic spine density in the corresponding cortical area, and a

decrease in sensory experience lowers the dendritic spine density. For example, there is an increase in dendritic spine density on hippocampal CAl pyramidal neurons[50] following spatial learning in adult rats. Enucleation of mouse eyes lowers the incidence of dendritic spines[51] along the apical shafts of visual cortex pyramidal cells. Based on this, it would be expected that blind rats have lower dendritic spine density unlike the results we obtained in our comparison between the visual cortex neurons of normally sighted and blind rats. It appears that while there is a strong correlation between synaptic plasticity and morphologic changes in spines, it is not yet known if these morphologic changes are necessary or sufficient[52,53] for functional plasticity. It is possible that the increased dendritic spine density we report here for neurons in the visual cortex of *rd* rats may be correlated or may be coincidental to the increased spontaneous activity seen in the visual cortex of *rd* rats.

The retinotopic cortical activity maps presented in this paper are the first published maps for epiretinal electrical stimulation of the retina in normally sighted versus blind rats. These results can be used as a baseline to investigate if and how retinotopy changes in *rd* rats with chronic electrical stimulation of the retina with epiretinal electrodes. A key question to answer would be whether or not the loss of retinotopic organization seen in *rd* rats is reversed by chronic electrical stimulation of the retina with epiretinal electrodes. In the case of cochlear implants, it has been shown that the loss of normal cochleotopic organization in the auditory cortex of deafened cats was almost completely reversed by chronic reactivation of the auditory pathway[54] with the use of an electronic cochlear prosthesis. It is an open question whether such reversal is possible with retinal prostheses. For our initial study of cortical mapping for acute stimulation of the retina, we chose four quadrants of the retina to stimulate because reliable positioning of the electrode with more precision would be difficult in this experiment. With a chronically implanted array, electrode position should remain stable. Repeating these cortical mapping experiments using electrode arrays for retinal stimulation as well as cortical recording will allow us to characterize cortical activation maps with higher resolution. Longitudinal studies, enabled by chronic implants, can answer questions related to the preservation or loss of retinotopy with retinal degeneration and chronic electrical stimulation. Another avenue of investigation will be to repeat the cortical mapping experiments with varying pulse parameters that avoid axonal stimulation. These future studies may allow us to better understand the interplay between threshold for retinal stimulation, duration of intervention, developmental timing of intervention, and cortical changes with and without chronic electrical stimulation of the retina.

Acknowledgments

The authors thank Drs. Artin Petrossians and Curtis Lee for the high-surface area Pt/Ir thin film coating used with some stimulation electrodes in this study; Prof. Michael Jakowec for advice and assistance for performing the golgi stain portion of the study; and Fernando Gallardo and Lina Flores for assistance during the animal surgeries. A subset of the results in this study have been reported[55,56] previously.

Supported by the National Science Foundation Grant numbers CBET-1353018 and CBET-1343193, and an unrestricted departmental grant to the USC Department of Ophthalmology from Research to Prevent Blindness.

Disclosure: **K. Nimmagadda**, None; **J.D. Weiland**, high surface area Pt/Ir electrodes (F)

References

1. Schuman SG, Koreishi AF, Farsiu S, Jung SH, Izatt JA, Toth CA. Photoreceptor layer thinning over drusen in eyes with age-related macular degeneration imaged in vivo with spectral-domain optical coherence tomography. *Ophthalmology*. 2009;116:488–496.
2. Medeiros NE, Curcio CA. Preservation of ganglion cell layer neurons in age-related macular degeneration. *Invest Ophthalmol Vis Sci*. 2001;42:795–803.
3. Soubrane G, Cruess A, Lotery A, et al. Burden and health care resource utilization in neovascular age-related macular degeneration: findings of a multicountry study. *Arch Ophthalmol*. 2007;125:1249–1254.
4. Lotery A, Xu X, Zlatava G, Loftus J. Burden of illness, visual impairment and health resource utilisation of patients with neovascular age-related macular degeneration: results from the

UK cohort of a five-country cross-sectional study. *Br J Ophthalmol*. 2007;91:1303–1307.
5. Curcio CA, Medeiros NE, Millican CL. Photoreceptor loss in age-related macular degeneration. *Invest Ophthalmol Vis Sci*. 1996;37:1236–1249.
6. Margalit E, Sadda SR. Retinal and optic nerve diseases. *Artif Organs*. 2003;27:963–974.
7. Leonard R, Gordon AR. *Statistics on Vision Impairment: A Resource Manual*. New York, NY: Research Institute of Lighthouse International; 2001.
8. Brown GC, Brown MM, Sharma S, et al. The burden of age-related macular degeneration: a value-based medicine analysis. *Trans Am Ophthalmol Soc*. 2005;103:173.
9. Sohocki MM, Daiger SP, Bowne SJ, et al. Prevalence of mutations causing retinitis pigmentosa and other inherited retinopathies. *Hum Mutat*. 2001;17:42.
10. Humayun MS, Prince M, de Juan E, et al. Morphometric analysis of the extramacular retina from postmortem eyes with retinitis pigmentosa. *Invest Ophthalmol Vis Sci*. 1999;40:143–148.
11. Humayun MS, de Juan E Jr, Weiland JD, et al. Pattern electrical stimulation of the human retina. *Vision Res*. 1999;39:2569–2576.
12. Marc RE. Injury and repair: retinal remodeling. *Encyclopedia of the Eye*. 2010;2:414–420.
13. Weiland JD, Walston ST, Humayun MS. Electrical stimulation of the retina to produce artificial vision. *Ann Rev Vis Sci*. 2016;2:273–294.
14. Hesse L, Schanze T, Wilms M, Eger M. Implantation of retina stimulation electrodes and recording of electrical stimulation responses in the visual cortex of the cat. *Graefes Arch Clin Exp Ophthalmol*. 2000;238:840–845.
15. Mandel Y, Goetz G, Lavinsky D, et al. Cortical responses elicited by photovoltaic subretinal prostheses exhibit similarities to visually evoked potentials. *Nat Commun*. 2013;4:1980.
16. Lorach H, Goetz G, Mandel Y, et al. Performance of photovoltaic arrays in-vivo and characteristics of prosthetic vision in animals with retinal degeneration. *Vision Res*. 2015;111:142–148.
17. Roux S, Matonti F, Dupont F, et al. Probing the functional impact of sub-retinal prosthesis. *Elife*. 2016;5.
18. Chader GJ. Animal models in research on retinal degenerations: past progress and future hope. *Vision Res*. 2002;42:393–399.
19. Gias C, Hewson-Stoate N, Jones M, Johnston D, Mayhew JE, Coffey PJ. Retinotopy within rat primary visual cortex using optical imaging. *Neuroimage*. 2005;24:200–206.
20. Paxinos G, Watson C. *The Rat brain in Stereotaxic Coordinates*. Burlington, MA: Elsevier Publishing; 2014.
21. Petrossians A, Whalen JJ, Weiland JD, Mansfeld F. Electrodeposition and characterization of thin-film platinum-iridium alloys for biological interfaces. *J Electrochem Soc*. 2011;158:D269–D276.
22. Ray A, Chan LLH, Gonzalez A, Humayun MS, Weiland JD. Impedance as a method to sense proximity at the electrode-retina interface. *IEEE Trans Neural Syst Rehabil Eng*. 2011;19:696–699.
23. Sekirnjak C, Hottowy P, Sher A, Dabrowski W, Litke AM, Chichilnisky EJ. Electrical stimulation of mammalian retinal ganglion cells with multielectrode arrays. *J Neurophysiol*. 2006;95:3311–3327.
24. Larkman AU. Dendritic morphology of pyramidal neurones of the visual cortex of the rat: III. Spine distributions. *J Comp Neurol*. 1991;306:332–343.
25. Petrossians A, Davuluri N, Whalen JJ, Mansfeld F, Weiland JD. Improved biphasic pulsing power efficiency with Pt-Ir coated microelectrodes. MRS Online Proceedings Library Archive. 2014;1621:249–257.
26. Frostig RD, Chen-Bee CH. Visualizing adult cortical plasticity using intrinsic signal optical imaging. In: Frostig RD, ed. *In Vivo Optical Imaging of Brain Function*, 2nd ed. Boca Raton, FL: CRC Press; 2009:1–32.
27. Weitz AC, Behrend MR, Lee NS, et al. Imaging the response of the retina to electrical stimulation with genetically encoded calcium indicators. *J Neurophysiol*. 2013;109:1979–1988.
28. Lorach H, Goetz G, Smith R, et al. Photovoltaic restoration of sight with high visual acuity in rats with retinal degeneration. *Nat Med*. 2015;21:476–482.
29. Ferreira S, Pereira AC, Quendera B, Reis A, Silva ED, Castelo-Branco M. Primary visual cortical remapping in patients with inherited peripheral retinal degeneration. *Neuroimage Clin*. 2017;13:428–438.
30. Baseler HA, Gouws A, Haak KV, et al. Large-scale remapping of visual cortex is absent in adult humans with macular degeneration. *Nat Neurosci*. 2008:14:649–655.
31. Lešták J, Tintěra J, Karel I, Svatá Z, Rozsíval P. Functional magnetic resonance imaging in patients with the wet form of age-related macular degeneration. *Neuroophthalmology*. 2013;37:192–197.
32. Baker CI, Dilks DD, Peli E, Kanwisher N. Reorganization of visual processing in macular

degeneration: replication and clues about the role of foveal loss. *Vision Res*. 2008:48:1910–1919.
33. Dilks DD, Baker CI, Peli E, Kanwisher N. Reorganization of visual processing in macular degeneration is not specific to the "preferred retinal locus". *J Neurosci*. 2009:29:2768–2773.
34. Greenberg RJ, Humayun MS, da Cruz L, et al. Five-year data from the Argus II Retinal Prosthesis System Clinical Trial. *Invest Ophthalmol Vis Sci*. 2015;56:754–754.
35. da Cruz L, Dorn JD, Humayun MS, et al. Five-year safety and performance results from the Argus II retinal prosthesis system clinical trial. *Ophthalmology*. 2016;123:2248–2254.
36. Boinagrov D, Pangratz-Fuehrer S, Suh B, Mathieson K, Naik N, Palanker D. Upper threshold of extracellular neural stimulation. *J Neurophysiol*. 2012;108:3233–3238.
37. Meng K, Fellner A, Rattay F, et al. Upper stimulation threshold for retinal ganglion cell activation. *J Neural Eng*. 2018;15:046012.
38. Chan LL, Lee EJ, Humayun MS, Weiland JD. Both electrical stimulation thresholds and SMI-32-immunoreactive retinal ganglion cell density correlate with age in S334ter line 3 rat retina. *J Neurophysiol*. 2011;105:2687–2697.
39. Davuluri NS, Nimmagadda K, Petrossians A, Humayun MS, Weiland JD. Strategies to improve stimulation efficiency for retinal prostheses. *Conf Proc IEEE Eng Med Biol Soc*. 2016;2016:3133–3138.
40. Lorach H, Lei X, Galambos L, et al. Interactions of prosthetic and natural vision in animals with local retinal degenerationinteractions of prosthetic and natural vision. *Invest Ophthalmol Vis Sci*. 2015;56:7444–7450.
41. Chen SJ, Mahadevappa M, Roizenblatt R, Weiland J, Humayun M. Neural responses elicited by electrical stimulation of the retina. *Trans Am Ophthalmol Soc*. 2006;104:252.
42. Jensen RJ, Rizzo JF. Activation of retinal ganglion cells in wild-type and rd1 mice through electrical stimulation of the retinal neural network. *Vision Res*. 2008;48:1562–1568.
43. Jensen RJ, Rizzo JF III. Activation of ganglion cells in wild-type and rd1 mouse retinas with monophasic and biphasic current pulses. *J Neural Eng*. 2009;6:035004.
44. O'Hearn TM, Sadda SR, Weiland JD, Maia M, Margalit E, Humayun MS. Electrical stimulation in normal and retinal degeneration (rd1) isolated mouse retina. *Vision Res*. 2006;46:3198–3204.
45. Suzuki S, Humayun MS, Weiland JD, et al. Comparison of electrical stimulation thresholds in normal and retinal degenerated mouse retina. *Jap J Ophthalmol*. 2004;48:345–349.
46. Stasheff SF. Emergence of sustained spontaneous hyperactivity and temporary preservation of OFF responses in ganglion cells of the retinal degeneration (rd1) mouse. *J Neurophysiol*. 2008;99:1408–1421.
47. Cho A, Ratliff C, Sampath A, Weiland J. Changes in ganglion cell physiology during retinal degeneration influence excitability by prosthetic electrodes. *J Neural Eng*. 2016;13:025001.
48. Borowska J, Trenholm S, Awatramani GB. An intrinsic neural oscillator in the degenerating mouse retina. *J Neurosci*. 2011;31:5000–5012.
49. Wang Y, Chen K, Xu P, Ng TK, Chan LL. Spontaneous neural activity in the primary visual cortex of retinal degenerated rats. *Neurosci Lett*. 2016;623:42–46.
50. Moser MB, Trommald M, Andersen P. An increase in dendritic spine density on hippocampal CA1 pyramidal cells following spatial learning in adult rats suggests the formation of new synapses. *Proc Natl Acad Sci U S A*. 1994;91:12673–12675.
51. Valverde P. Apical dendritic spines of the visual cortex and light deprivation in the mouse. *Exp Brain Res*. 1967;3:337–352.
52. Yuste R, Bonhoeffer T. Morphological changes in dendritic spines associated with long-term synaptic plasticity. *Ann Rev Neurosci*. 2001;24:1071–1089.
53. Alvarez VA, Sabatini BL. Anatomical and physiological plasticity of dendritic spines. *Ann Rev Neurosci*. 2007;30:79–97.
54. Fallon JB, Irvine DR, Shepherd RK. Cochlear implant use following neonatal deafness influences the cochleotopic organization of the primary auditory cortex in cats. *J Comp Neurol*. 2009;512:101–114.
55. Nimmagadda K, Weiland JD. Retinotopy within rat primary visual cortex in response to electrical stimulation of the retina. Paper presented at: 8th International IEEE/EMBS Conference on Neural Engineering (NER); May 25–28, 2017; Shanghai, China.
56. Nimmagadda K, Weiland J. Electrical stimulation of rat retina elicits retinotopic cortical electrophysiology activity with a dose response characteristic. *Invest Ophthalmol Vis Sci*. 2015;56:774.